

Adsorption of aurocyanide complexes onto carbonaceous matter from preg-robbing Goldstrike ore

Philip A. Schmitz^a, Saskia Duyvesteyn^b, William P. Johnson^{a,*},
Larry Enloe^c, Jacques McMullen^d

^a Department of Geology and Geophysics, 135 S. 1460 E. Room 719, University of Utah, Salt Lake City, UT 84112-0111, USA

^b Department of Metallurgical Engineering, 135 S. 1460 E. Room 412, University of Utah, Salt Lake City, UT 84112-0114, USA

^c Barrick Goldstrike Mine Incorporated Metallurgical Services, Carlin, NV, 89822, USA

^d Barrick Gold Corporation Inc. Royal Bank Plaza, Southtower, Suite 2700, 200 Bay Street, PO Box 119, Toronto, Canada, M5J 2J3

Received 18 August 2000; received in revised form 14 February 2001; accepted 26 February 2001

Abstract

Aurocyanide complex adsorption by naturally occurring carbon in Goldstrike ore has been implicated in a form of gold refractoriness known as “preg-robbing”. The aim of this work was to establish a relationship between the aurocyanide uptake capacity of Goldstrike ore carbonaceous matter and the preg-robbing behavior of the parent ore. The effect of varying contact time between the aqueous gold–cyanide and the carbonaceous matter on the uptake of aurocyanide complexes was also investigated. In column adsorption experiments, the adsorbed gold concentration from 100 mL of a gold–cyanide solution depended on the flow rate of the solution. The concentration of adsorbed gold increased with solution flow rate, reaching a maximum concentration at a flow rate of approximately 0.05 mL/min. As solution flow rate increased to more than 0.05 mL/min, the concentration of gold adsorbed on the carbon decreased. Desorption of adsorbed gold into 75-mL sodium cyanide solution also depended on solution flow rate. Maximum desorption of gold occurred at a flow rate of approximately 0.14 mL/min. The gold adsorbed at the lowest and highest flow rates was more slowly desorbed than the additional gold adsorbed at the intermediate flow rates. The concentration of gold remaining on the carbon after desorption at 0.14 mL/min correlated to the amount of gold adsorbed at the highest and lowest flow rates in the adsorption experiments. This amount of slowly desorbed gold correlated to the preg-robbing behavior of the ore, whereas the amount of additional adsorbed gold (i.e., gold adsorbed at intermediate flow rates) was similar for all of the ores. For all of the carbonaceous matters studied, the concentration of gold sorbed in both batch and column experiments increased after autoclaving. © 2001 Elsevier Science B.V. All rights reserved.

1. Introduction

Carbonaceous gold ores from Barrick Goldstrike Mines (BGMI) suffer from two forms of refractori-

ness. Over 50% of the gold is encapsulated within the pyrite rings of arsenian framboidal pyrite [1–4] and is not amenable to leaching [5]. Consequently, autoclaving is used as a pretreatment process to release elemental gold from the sulfide matrix [6]. However, some Goldstrike ores also suffer from a form of refractoriness known as “preg-robbing”. Preg-robbing was the term first used by Smith [7] to

* Corresponding author. Tel.: +1-801-581-5033.
E-mail address: wjohnson@mines.utah.edu (W.P. Johnson).

describe the loss of gold from pregnant cyanide solutions during the processing of carbonaceous ores.

During processing of Goldstrike ore, cyanide ions complex elemental gold to form aqueous $\text{Au}(\text{CN})_2^-$ complexes. A carbon-in-leach (CIL) circuit removes the gold–cyanide complex from the aqueous solution by adsorption onto coarse-grained commercial activated carbon. The loaded commercial activated carbon is then separated by screening, and gold is stripped from the commercial activated carbon using the Zadra method [6]. However, during the processing of preg-robbing carbonaceous ores, a significant fraction of the gold present in the ore is not adsorbed by the commercial activated carbon. It has been presumed that gold not recovered from commercial activated carbon was adsorbed onto the naturally occurring fine-grained organic carbon present in Goldstrike ore, and is subsequently discarded with the ore tailings, since this fine grained carbon is not retained by screening [8,9].

Roasting preg-robbing carbonaceous ores increases gold recovery. While roasting of carbonaceous ore is an alternative to autoclaving, additional information is, however, necessary to assess whether the ore should be routed to the autoclave or the roaster. BGMI currently uses different methods to determine the preg-robbing nature of the ore, since significant variation exists in the preg-robbing behavior of Carlin trend carbonaceous ores [7]. One simple method used by BGMI is a “preg-robbing” test. In the preg-robbing test, a percent preg-robbing value (%PR) is obtained by measuring the change in solution of gold concentration after contacting a gold–cyanide solution with a known mass of ore in batch for 15 min [5,10]. The ability of the preg-robbing test to predict the preg-robbing behavior of the ore during CIL processing is limited, since no commercial activated carbon is added during the test. Hence, during preg-robbing tests, the naturally occurring carbon present in the ore does not compete with commercial carbon for aqueous gold complexes, as it does during CIL processing. As a result, BGMI also determines the refractoriness of Goldstrike ore, due to both carbon and sulfide encapsulation refractoriness, utilizing a bench-top autoclave, followed by carbon-in-leach (BTAC–CIL) test. In the BTAC–CIL test, autoclaved ore and commercial

activated carbon are equilibrated in a sodium cyanide solution for 16 h, and the recovery of gold (%REC) is determined by dividing the mass fraction of gold recovered on the commercial activated carbon by the mass of gold in the head ore, as determined by fire assay [5,10]. The ability of the BTAC–CIL test to predict the preg-robbing behavior of the ore during processing is also limited since the value obtained for %REC depends in part on the oxidation efficiency of the bench-top autoclave used in the test relative to the continuous autoclave used during industrial processing. Although the preg-robbing behavior of the ores used in this study was quantified by %PR and %REC, the preg-robbing behavior during processing of some ores cannot be accurately predicted using these tests due to the previously described limitations in the preg-robbing and BTAC–CIL tests. As a result, BGMI recently developed a “bleach leach” test, in which addition of hypochlorite solution to the standard preg-robbing test has been empirically shown to more accurately assess the “true” preg-robbing behavior of the ore [11]. The more accurate assessment of the true preg-robbing behavior of the ore by the bleach leach method relative to %PR, is thought to be due to the deactivation of weakly adsorbing domains in the naturally occurring carbon that yield their gold to commercial activated carbon during processing [12]. The development of the bleach leach test is recent and, therefore, was not used to assess the preg-robbing behavior of the ores in this study.

Since it has been hypothesized that the preg-robbing behavior of Carlin trend ore is the result of aurocyanide complex adsorption by naturally occurring carbon during processing [8,9], an acid demineralization process was used to remove silicate and carbonate mineral phases to concentrate the remaining phases (carbon, sulfides, etc.) into a material referred to in this paper as carbonaceous matter (CM). The focus of this study was to determine whether the aurocyanide complex uptake capacity of CM from autoclaved Goldstrike ore correlated to the preg-robbing behavior of the parent ore. Since %PR is determined from non-autoclaved ore, and %REC is determined from autoclaved ore, tests were also performed to determine the effect of autoclaving on the aurocyanide complex uptake behavior of the CM.

2. Background

Commercial activated carbon is a generic term referring to a family of carbonaceous materials obtained from coconut shells, coal, peach pits, etc., which are heated in the presence of an oxidizing agent to remove the more reactive functional groups from the aromatic carbon structure. The remaining carbon skeleton is composed of featureless aromatic carbon rings with an overall structure similar to that of graphite [13]. Naturally occurring carbon in Goldstrike ore is also composed of featureless aromatic rings and has been shown to be of high maturity with a rank equal to or greater than anthracite coal [3,14–16]. Stenebråten et al. [10] suggest that naturally occurring organic carbon in preg-robbing Goldstrike ore is chemically equivalent to commercial activated carbon activated at temperatures above 750°C.

Graphite, commercial activated carbon, and mature natural organic carbon are each composed of stacked sheets of aromatic carbon rings, referred to as microcrystallites. The maturity of the carbon is directly related to the length of the microcrystallite perpendicular to the aromatic planes (L_c), and inversely related to the distance between aromatic sheets (d-spacing). The adsorption of aurocyanide complexes by commercial activated carbon has been shown to be inversely related to the microcrystallite L_c and is directly related to microcrystallite d-spacing [17]. Likewise, the preg-robbing behavior of Goldstrike ore has been shown to be inversely related to the L_c and directly related to the d-spacing of naturally occurring carbon in Goldstrike ore [5,10].

Another similarity between Goldstrike ore CM and commercial activated carbon is the lack of gold retention during ammoniacal thiosulfate leaching [5]. Following ammoniacal thiosulfate leaching, the CM retains less than 10% of the gold initially present on the CM, regardless of the preg-robbing behavior of the parent ore [5]. This result is consistent with the low adsorption of gold–thiosulfate complexes by commercial activated carbon [18]. Chemical and physical similarities between the naturally occurring carbon in Goldstrike ore and commercial activated carbon suggest that preg-robbing during ore processing results from the retention of gold complexes on the naturally occurring carbon by a mechanism simi-

lar to the adsorption of aurocyanide complexes on commercial activated carbon [5,8–10].

The various mechanisms of aurocyanide complex adsorption by commercial activated carbon can be summarized as one of the following mechanisms: reduction of the gold in the cyanide complex to metallic gold, adsorption as an ion-pair, or the precipitation of Au(CN) as a result of chemical degradation of the aurocyanide complex [13]. Recent theories suggest that there is no chemical change in the aurocyanide complex after adsorption onto commercial activated carbon surfaces [19–24], and these theories favor adsorption as an ion-pair as the dominant mechanism of gold uptake. Investigators have also suggested that sites responsible for aurocyanide complex adsorption are either concentrated at structural defects along the edges of microcrystallites [24,25] or along the basal planes of the graphitic sheets [21,22]. Comprehensive reviews of these theories of aurocyanide complex adsorption are given in Adams et al. [19,20], McDougal et al. [23], and Sibrell [26].

Recent studies of aurocyanide complex adsorption onto commercial activated carbon indicate that weakly and strongly adsorbing domains occur. Irreversible and reversible components of gold adsorption have been observed in batch experiments [27,28]. At relatively low equilibrium aqueous gold concentrations, gold adsorption was irreversible under the conditions of the experiments. Higher equilibrium aqueous and adsorbed gold concentrations resulted in a reversible component of adsorbed gold [27,28].

3. Methods

3.1. Sample preparation

BGMI supplied four dry-ground samples (80%–200 mesh) of Goldstrike ore with various preg-robbing behaviors. A fire assay was performed on each of the samples to determine the initial gold content of the ore. In addition, the carbon and sulfide contents of the ores were determined by LECO analysis, and %PR and %REC were determined by BGMI Metallurgical Services (Table 1). A portion of each

Table 1

Chemical composition of the Goldstrike ores used in this study. LECO analysis for sulfur and carbon and fire assay for gold content. OPT refers to ounces per ton

Sample Source	Sample ID	%REC	%PR	Au (OPT)	%S (sulfide)	%C (organic)
BR-22	BR-22	0.0	100.0	0.088	1.45	3.8
6th West	6th West	8.3	53.0	0.084	2.4	0.8
PR-1G	PR-1G	53.6	32.0	0.321	1.77	1.1
Betze COF composite	BTZ#3	92.5	< 5.0	0.326	1.67	0.5
8/26/97–9/25/97						

ore sample was autoclaved for 1 h at 240°C with an oxygen overpressure of 880 kPa.

The carbon in the ore was concentrated by the removal of quartz and other minerals, according to a demineralization procedure described in Stenebråten et al. [10]. Hydrochloric acid was used to remove the carbonates, and repeated digestions in hydrofluoric acid were used to dissolve quartz. In addition to concentrating the carbon, the demineralization procedure concentrated the sulfides and gold, and produced fluorite [5]. A portion of the resulting CM from each parent ore was sent to BGMI Metallurgical Services for LECO analysis and fire assay (Table 2).

3.2. Adsorption experiments

Although the primary factor controlling the preg-robbing behavior of Goldstrike ore was shown to be the microcrystallinity of the carbon, the carbon content of the ore also influenced the preg-robbing behavior of the ore [10], and gold adsorption by the associated CM. In preliminary adsorption tests, a

constant mass of 50 mg of CM was used to adsorb gold from 0.5 g/L NaCN solution containing 5 ppm gold (pH 10.8). Fig. 1 shows a direct correlation between the total mass of gold adsorbed by the CM and the carbon content of the CMs, indicating that the adsorption of gold–cyanide complexes by the CM was directly related to the carbon content of the CM; as a result, the mass of CM used in all subsequent experiments was varied, so that the carbon content of each sample was held constant at 10 mg.

Column tests involved placing sufficient CM in a syringe filter (Swinnex 0.22 μm) to obtain 10 mg of carbon. A modified column system was created by pumping fluid from a 10-mL syringe, used as a fluid reservoir, through the syringe filter as was described in Schmitz et al. [5]. One hundred milliliters of solution containing 10 ppm Au and 2.0 g/L NaCN (adjusted with NaOH to pH 10.8) was pumped

Table 2

Chemical composition of the carbonaceous matter from demineralized Goldstrike ore. LECO analysis for sulfur and carbon and fire assay for gold content. OPT refers to ounces per ton

Sample ID	Au (OPT)	%C (organic)	%S (sulfide)
BR-22	0.82	36.8	4.6
Autoclaved BR-22	3.12	33.4	0.2
PR-1G	5.50	18.8	21
Autoclaved PR-1G	8.64	23.6	4.6
6th West	2.12	16.6	28.2
Autoclaved 6th West	5.72	43.0	9.0
BTZ#3	6.54	10.0	42.0
Autoclaved BTZ#3	14.78	23.8	8.6

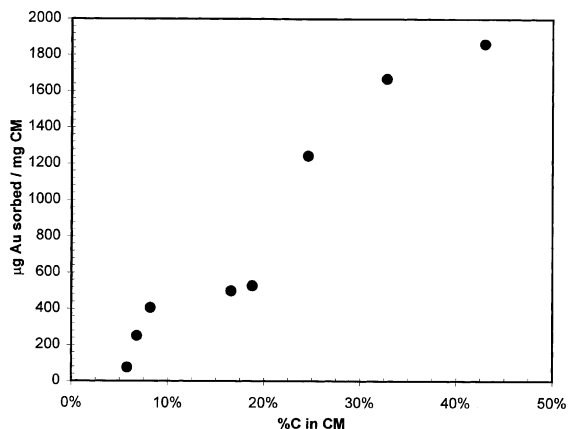


Fig. 1. Concentration of gold adsorbed onto 50 mg of Goldstrike CM vs. the carbon content of the CM. Gold adsorption was performed in column experiments at a flow rate of 0.05 mL/min with 5 ppm Au in 2.0 g/L NaCN at pH 10.8.

through the filter. A peristaltic pump (Cole Palmer, Digi-Static 7526-00) was used at flow rates ranging from 0.05–2.0 mL/min, and a syringe pump (Carnegie Medicin AB, CMA-100) was used for flow rates ranging from 0.008 to 0.05 mL/min. Both the peristaltic pump and syringe pump were used at a flow rate of 0.05 mL/min to verify continuity between the two pumping conditions. At 0.05 mL/min, the difference in the concentration of gold adsorbed using the two different pumping systems was less than 5%. Aliquots of the effluent gold solution were collected and analyzed for solution gold concentration using Inductively Coupled Plasma Atomic Emission Spectroscopy (ICP-AES) (Perkin Elmer Plasma 400) at a wavelength of 242.795 nm.

In addition to column adsorption tests, batch adsorption tests were also performed. In batch tests, CM (10 mg C) from both autoclaved and non-autoclaved ores were equilibrated with the gold–cyanide solution (10 ppm Au and 2.0 g/L NaCN, pH 10.8) in a 20-mL scintillation vial, rotated at 20 revolutions per minute for 72 h (Glas-col Laboratory Products lab rotator). After equilibration, the solution was filtered using a syringe filter, and the filtrate was analyzed for aqueous gold concentration using ICP-AES.

3.3. Determination of adsorbed gold concentration

During adsorption tests, solubilization of gold, which was initially present in the CM, caused the concentration of gold–cyanide complexes in solution to increase relative to what was added as a spike. Since 100% of gold initially present in the CMs from autoclaved ores and 40% of gold initially present in CMs from non-autoclaved ores was amenable to leaching [5], the total mass of gold to which the CM was exposed could be calculated by adding a fraction of the gold mass initially present (1.0 and 0.4 for autoclaved and non-autoclaved, respectively) to the aqueous gold mass in the contact solution. The mass of gold adsorbed by the CM at a given point during the experiment was determined by subtracting the mass of gold obtained in the effluent aliquots up to that point from the total mass of gold to which the CM was exposed. The concentration of gold adsorbed by the carbon was expressed per mass of carbon in the CM (10 mg).

3.4. Desorption experiments

Desorption of gold adsorbed by CMs from autoclaved ores was also performed. Multiple samples of a given CM were loaded with similar amounts of gold by introducing 100 mL of gold–cyanide solution at a flow rate of 0.10 mL/min, using the procedure outlined for the column adsorption experiments. Desorption of gold complexes from the CM was achieved by pumping sodium cyanide solution (2.0 g/L NaCN, pH 10.8) through the syringe filter containing the gold-loaded CM. Since steady-state values for gold desorption were obtained with 75 mL of cyanide solution at the slowest flow rates, this volume of cyanide solution was used in all desorption experiments. The effluent solution was collected in 5–20 mL aliquots and analyzed for gold in solution using ICP-AES. The desorbed gold mass (concentration multiplied by aliquot volume) was normalized to the mass of carbon (10 mg) and referenced to the initial mass of gold adsorbed, as previously described.

4. Results and analyses

4.1. Adsorption of gold complexes onto naturally occurring organic carbon

Fig. 2 shows gold adsorbed from 100 mL of 10 ppm gold solution as a function of time for different solution flow rates for CM from one representative ore sample (6th West). At the lowest flow rate studied (0.008 mL/min), the concentration of gold adsorbed by the carbon reached a plateau, indicating that at this flow rate, a steady-state was achieved between the adsorbed gold on the CM and the aqueous gold–cyanide. As the solution flow rate increased, the concentration of gold adsorbed from 100 mL of solution increased, reaching a maximum at 0.05 mL/min. As flow increased above 0.05 mL/min, the adsorption curves steepened, but the total concentration of gold adsorbed from 100 mL of solution decreased (Fig. 2).

4.2. Desorption of adsorbed gold complexes

While it is recognized that elution procedures utilizing elevated temperatures and a variety of lixi-

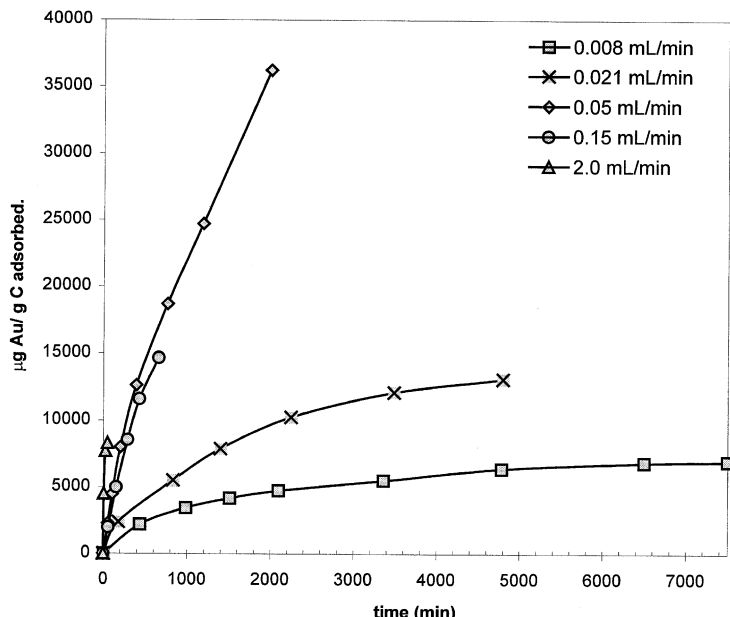


Fig. 2. Concentration of gold adsorbed from 10 ppm gold–cyanide (2.0 g/L NaCN, pH ~ 10.8) solution onto CM demineralized from Goldstrike ore 6th West as a function of total experiment time for column experiments at flow rates of 0.008, 0.021, 0.05, 0.015 and 2.0 mL/min for a constant 100 mL volume of solution.

vants can effectively recover adsorbed gold from carbon, gold desorption was determined under the experimental conditions of the adsorption experiments ($23 \pm 2^\circ\text{C}$) (2.0 g/L NaCN, pH 10.8). A washing step to remove entrained solution was not employed prior to desorption since the mass of gold (0.5 μg) present in the pore space in the carbonaceous matter (maximum 0.1 cm³) would yield a 0.1 ppm gold concentration in the 5-mL aliquot. This concentration was below the detection limit of the equipment used and was less than 2% of the lowest concentration measured in any of the first aliquots.

Fig. 3 shows the concentration of gold desorbed from carbon into 75 mL of cyanide solution as a function of time (flow rate) for CM from PR-1G. As was observed for the adsorbed gold concentrations in the adsorption experiments, the concentration of gold remaining on the carbon after desorption with 75 mL of NaCN solution varied with flow rate. Desorption of gold from the carbon increased (greater percentage of adsorbed gold was removed) with increasing flow rate, reaching a minimum gold concentration on the carbon at a flow rate of ~ 0.14 mL/min. As

desorption flow rate increased beyond 0.14 mL/min, the desorption of gold from carbon decreased (a lesser percentage of adsorbed gold was removed), approaching the gold concentration remaining at the two slowest flow rates.

4.3. Comparison of adsorption and desorption experiments

Fig. 4 shows cumulative adsorbed gold concentrations resulting from contact of naturally occurring organic carbon with 100 mL of solution. Gold adsorption at ~ 0.09 mL/min was repeated multiple times (4–16) for each CM and yielded standard errors of less than 5%. In Fig. 4, gold adsorption was expressed as the concentration of gold on the carbon after the passage of 100 mL of 10 ppm Au in 2.0 g/L NaCN solution at a given flow rate. As was observed for 6th West (Fig. 2), the concentration of gold remaining on the carbon for all of the CMs studied, increased with flow rate until it reached a maximum near 0.05 mL/min, and then decreased as the flow rate further increased. The cumulative gold

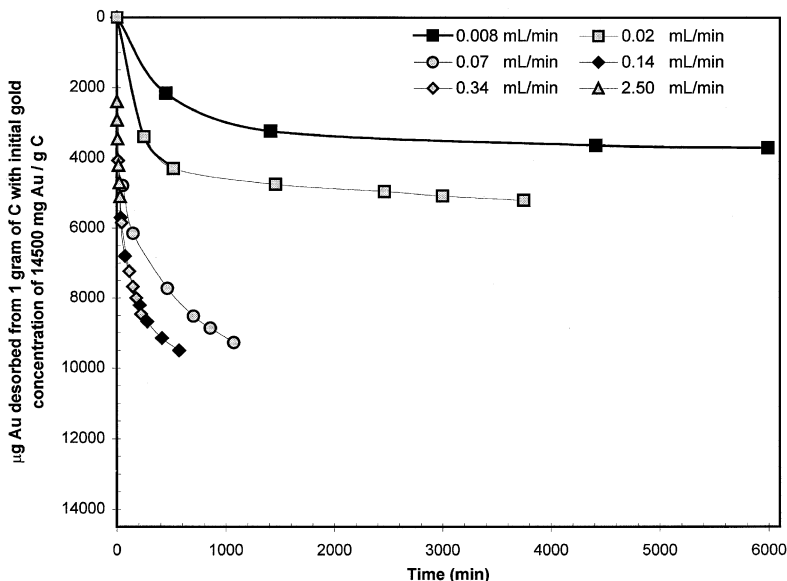


Fig. 3. Mass of gold desorbed into 75 mL of 2.0 g/L NaCN solution per gram of carbon from CM demineralized from Goldstrike ore PR-1G as a function of time at flow rates of 0.008, 0.02, 0.07, 0.14, 0.34, 2.5 mL/min.

concentration achieved on the carbon at the fastest flow rates was similar to that achieved at the slowest flow rates. For all CMs, the maximum adsorbed gold concentrations occurred at an intermediate flow rate.

During the adsorption experiments, the solution volume was held constant at 100 mL while the flow rate was varied; thus, the independent variable controlling the total concentration of adsorbed gold was the exposure time of the carbon to the aqueous gold solution. As a result, the shape of and variation in the curves shown in Fig. 2 was due to kinetic differences in the transfer of aqueous gold to and from the carbon. The overall concentration of gold adsorbed by the carbon is the difference between mass transfer of gold from the aqueous phase to the carbon ($Aq \rightarrow C$) and mass transfer of gold from the carbon to the aqueous phase ($C \rightarrow Aq$).

Fig. 4 also schematically shows the expected relative contributions of $C \rightarrow Aq$ and $Aq \rightarrow C$ to overall gold adsorption, compared to the magnitude of the flow rate, as illustrated by vectors representing the magnitudes of $Aq \rightarrow C$, $C \rightarrow Aq$, and flow rate (advective transport). Specifically, the vectors $Aq \rightarrow C$ and $C \rightarrow Aq$ represent the rate of gold mass transfer, which is equal to a kinetic rate constant multiplied by the corresponding gold concentration, from solu-

tion to carbon and from carbon to solution, respectively, after contact of the carbon with 100 mL of gold–cyanide solution. During adsorption at the slowest flow rate (0.008 mL/min), a steady-state gold concentration on the carbon was attained after some initial gold adsorption as shown by the plateau in Fig. 2. Hence, after initial gold adsorption, the relative contributions of $Aq \rightarrow C$ and $C \rightarrow Aq$ were equal and were not kinetically limited. As the flow rate increased to 0.05 mL/min, the net adsorption of gold from 100 mL of solution increased, indicating that either an increase in $Aq \rightarrow C$ or a decrease in $C \rightarrow Aq$ occurred. Had an increase in $Aq \rightarrow C$ occurred, a steady-state would have been preserved, since neither $Aq \rightarrow C$ nor $C \rightarrow Aq$ would have been kinetically limited (since neither was kinetically limited at the lower flow rate). Since steady-state was not preserved as flow rate increased (no plateau was achieved), the increased net gold transfer to carbon must have resulted from decreased $C \rightarrow Aq$. As flow rate increased above 0.05 mL/min, the net adsorption of gold from 100 mL of solution decreased, presumably due to kinetic limitations in $Aq \rightarrow C$. This is shown schematically in Fig. 4 where the advective transport vector exceeds the $Aq \rightarrow C$ vector at flow rates greater than 0.05 mL/min.

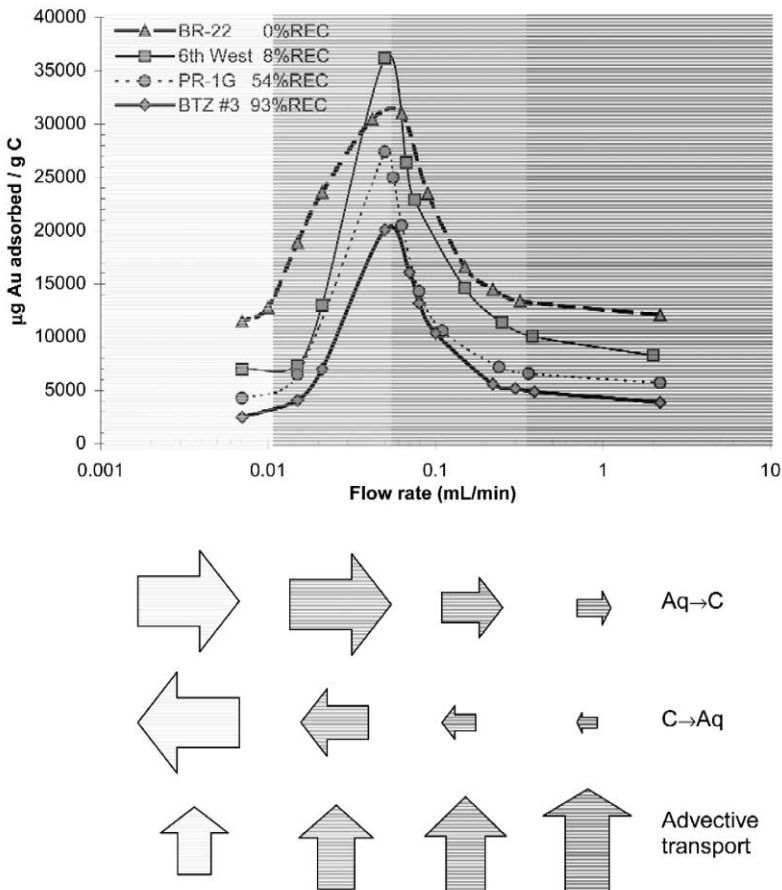


Fig. 4. Concentration of gold adsorbed at room temperature ($\sim 23^\circ\text{C}$) from 100 mL of 10 ppm gold–cyanide (2.0 g/L NaCN, pH ~ 10.8) solution onto four Goldstrike CMs containing 10 mg of carbon in column adsorption experiments as a function of column flow rate. For different flow regions, arrows schematically represent the total mass transfer of gold to and from the carbon, as well as through the column via advective transport.

Fig. 5 shows the effects of varying flow rate on gold desorption from a given mass of gold-loaded carbon. Desorption data at 0.008 mL/min was not obtained for BR-22 and BTZ#3 due to experimental difficulties. In Fig. 5, gold desorption is expressed as the concentration of gold remaining on the carbon after the passage of 75 mL of a 2 g/L NaCN solution at a given flow rate. As was observed for PR-1G (Fig. 3), the concentration of gold remaining on the carbon decreased with increasing flow rate until reaching a minimum at 0.14 mL/min, and then increased with increasing flow rate for CMs from all ores that were studied.

Fig. 5 also shows the expected contributions of $\text{C} \rightarrow \text{Aq}$ and $\text{Aq} \rightarrow \text{C}$ relative to the solution flow rate based on the results of the desorption experiments. The vectors $\text{C} \rightarrow \text{Aq}$ and $\text{Aq} \rightarrow \text{C}$ represent the rate of gold mass transfer from carbon to solution and from solution to carbon, respectively, after contact of the gold-loaded carbon with 75 mL of cyanide solution. At the lowest desorption flow rate (0.008 mL/min), the initial desorption of gold was followed by steady-state conditions (i.e., a plateau was achieved) (Fig. 3), indicating that $\text{Aq} \rightarrow \text{C}$ and $\text{C} \rightarrow \text{Aq}$ were equal in magnitude. At flow rates above 0.008 mL/min, the $\text{Aq} \rightarrow \text{C}$ and $\text{C} \rightarrow \text{Aq}$ vectors are

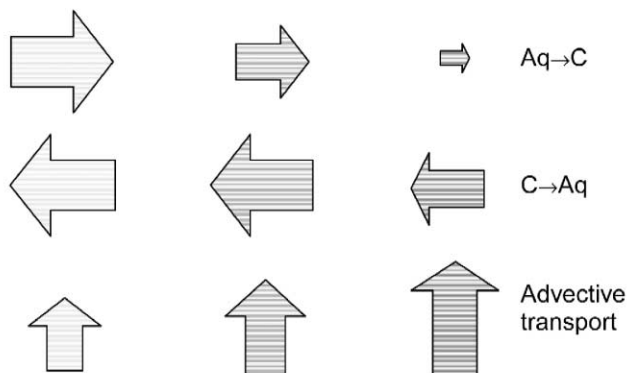
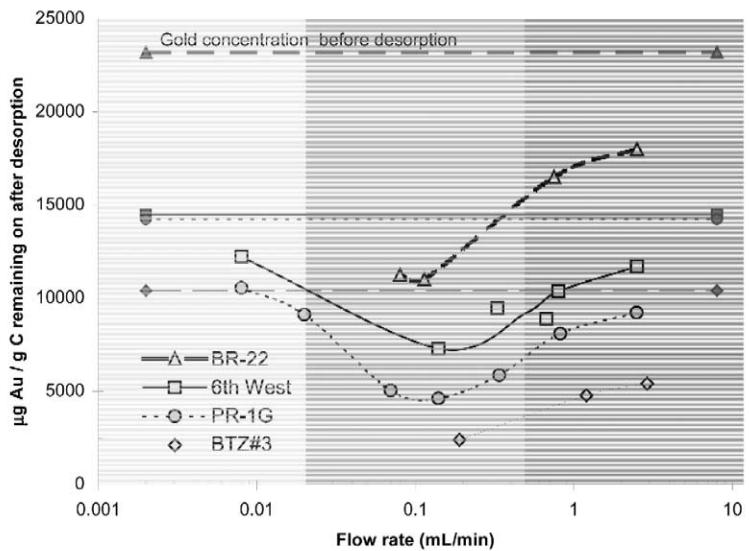


Fig. 5. The concentration of gold remaining on the carbon (curved lines) relative to initial gold concentrations (horizontal lines) after room temperature ($\sim 23^\circ\text{C}$) desorption of gold into 75 mL of 2.0 g/L NaCN solution for four Goldstrike ores as a function of flow rate. Prior to desorption, CMs were loaded with gold by adsorption from 10 ppm gold–cyanide (2.0 g/L NaCN, pH ~ 10.8) solution (~ 0.1 mL/min). For different flow regions, arrows schematically represent the total mass transfer of gold to and from the carbon as well as through the column via advective transport.

shown as being unequal since steady-state was not attained (i.e., a plateau was not achieved) (Fig. 3). As desorption flow rate increased to 0.14 mL/min, overall desorption of gold from the carbon increased due to either an increase in $\text{C} \rightarrow \text{Aq}$, or a decrease in $\text{Aq} \rightarrow \text{C}$. Had $\text{C} \rightarrow \text{Aq}$ increased, steady-state would have been preserved since neither $\text{Aq} \rightarrow \text{C}$ or $\text{C} \rightarrow \text{Aq}$ would have been kinetically limited (since neither were kinetically limited at the lower flow rate). Therefore, $\text{Aq} \rightarrow \text{C}$ decreased with increasing flow

rate, as shown in Fig. 5 by the greater magnitude of the advective transport vector relative to $\text{Aq} \rightarrow \text{C}$. At flow rates above 0.14 mL/min, desorption of gold from the carbon decreased (Fig. 5). Decreased desorption at flow rates above 0.14 mL/min can be presumed to be due to decreased $\text{C} \rightarrow \text{Aq}$, since $\text{Aq} \rightarrow \text{C}$ became kinetically limited at lower flow rates.

At the lowest flow rates during the adsorption experiments, the adsorbed gold concentration repre-

sented adsorption under conditions where neither $C \rightarrow Aq$ nor $Aq \rightarrow C$ were kinetically limited. At higher flow rates, $C \rightarrow Aq$ became kinetically limited and the adsorbed concentration increased. At still higher flow rates, $Aq \rightarrow C$ became kinetically limited and the adsorbed concentration decreased. At these highest flow rates in the adsorption experiments, greater solution volume (than 100 mL) would have been required to further increase the adsorbed gold concentration. These results suggest that the component of adsorbed gold achieved at the lowest and highest flow rates in the adsorption experiments were kinetically favored over the additional component of adsorption achieved at the intermediate flow rates. Likewise, further decreases in the concentration of adsorbed gold remaining at the end of the desorption experiments would have required larger solution volumes (than 75 mL). The minimum adsorbed gold concentrations (maximum stripping) achieved during desorption experiments, were achieved at the intermediate flow rates.

Comparison of the minimum gold concentrations achieved during desorption experiments to the kinetically favored adsorbed gold concentration achieved at the lowest flow rate during adsorption experiments (Fig. 6) shows that the two concentrations are well correlated ($r^2 = 0.994$), with a slope almost equal to unity. This result suggests that under conditions of

minimum loading during adsorption and maximum stripping during desorption, there remains an adsorbed gold concentration, which is kinetically favored. That the slope is slightly less than unity may be due to the different solution volumes used in the desorption experiments (75 mL) vs. the adsorption experiments (100 mL). This kinetically favored component of gold adsorption can be considered strongly adsorbed relative to the additional component of gold adsorption, which will be referred to as weakly adsorbed.

As described earlier, gold adsorption by commercial activated carbon has been proposed to occur by both “irreversible” and “reversible” mechanisms [27,28]. Given the similarities between commercial activated carbon and the natural carbon in these ores, it seems reasonable that gold–cyanide complex uptake by the natural carbon would also involve strong and weak components of adsorption. The results from this study suggest that strong aurocyanide adsorption to naturally occurring organic carbon is kinetically favored over weak adsorption, consistent with the observations made by Lagerge et al. [27,28], who identified limited irreversible adsorption of aurocyanide complexes that occurred prior to reversible adsorption to commercial activated carbon.

Fig. 7(a) shows a direct correlation between the strongly adsorbed gold concentration on CM from a given ore, and the associated %PR. Fig. 7(b) shows an inverse correlation between the strongly adsorbed gold concentration and %REC. These correlations suggest that this strongly adsorbed gold concentration may be the component of adsorption that was measured by the preg-robbing (%PR) and BTAC–CIL (%REC) tests for these ores. Table 3 shows the maximum concentration of gold that could have been adsorbed by the carbon (gold mass initially present in the ore plus any mass added during the test) during preg-robbing and BTAC–CIL tests performed on the ores used in this study. It should be noted that since only about 50% of the initial gold content of non-autoclaved Goldstrike ore is amenable to sodium cyanide leaching (Chryssoulis et al. [2] and Schmitz et al. [5]), the maximum concentration of gold that could have been adsorbed by the carbon in the preg-robbing tests is actually lower than what is reported in the table. This adsorbed concentration was less than that required to saturate the strongly

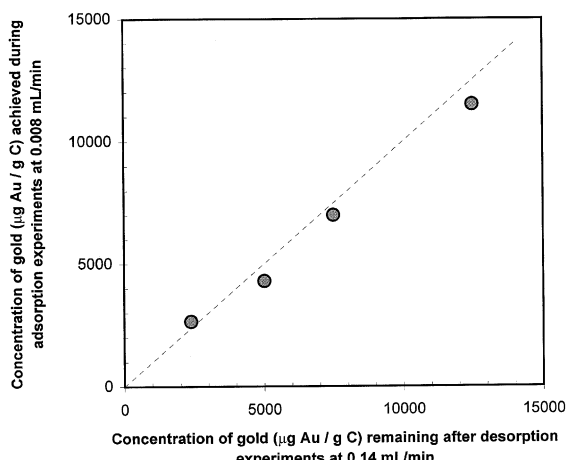


Fig. 6. Concentration of gold adsorbed during column adsorption experiments (10 ppm Au, 2.0 g/L NaCN, pH 10.8) at 0.008 mL/min compared to the concentration of gold remaining after desorption into 75 mL of 2.0 g/L sodium–cyanide solution at the flow rate of maximum desorption (~ 0.14 mL/min).

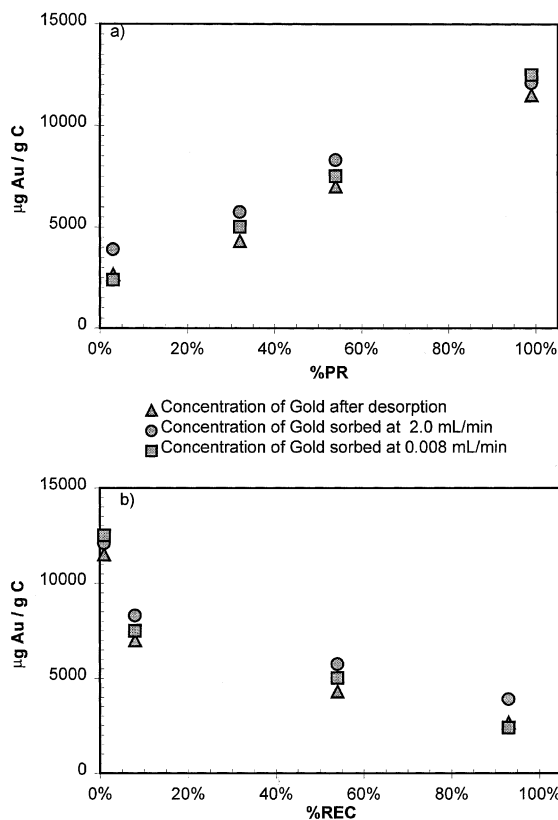


Fig. 7. Concentration of gold adsorbed at room temperature ($\sim 23^\circ\text{C}$) from 10 ppm gold-cyanide (2.0 g/L NaCN, pH ~ 10.8) by CM obtained from non-autoclaved Goldstrike ore compared to gold adsorption by CM obtained by demineralizing the same Goldstrike ores after bench-top autoclaving done by BGMI. Adsorption experiments were conducted in columns at flow rates of 0.06 and 2.0 mL/min and in a 72-h batch experiment.

adsorbed component of adsorption, further corroborating the correlations shown in Fig. 7.

4.4. Effect of autoclaving on the adsorption of aurocyanide complexes by the CM

Fig. 8 shows the effect of autoclaving on gold adsorption by the carbon. CM from autoclaved ore (open symbols) consistently showed higher gold adsorption than the CMs from corresponding non-autoclaved ore (closed symbols), regardless of whether the experimental format was batch (triangles) or column (at 0.06 and 2.0 mL/min, circles and squares, respectively). Previous studies of the effects of autoclaving on the chemistry of the CM [5,15] showed that the FT-IR spectra of strongly preg-robbing ores gained a new peak at 1720 cm^{-1} after autoclaving. This new peak was attributed to carboxylate or related functionality. Contrary to the observations made in this study, passivation of Carlin trend carbons in previous studies (by autoclaving or sodium hypochlorite treatment) resulted in the formation of a peak at 1720 cm^{-1} that correlated to a reduction in the preg-robbing behavior [26]. At present, we have no explanation for these seemingly contradictory results.

Gold–cyanide complex adsorption by commercial activated carbon is thought to occur along edge defects in the microcrystallite [24,26]. Since the behavior of naturally occurring carbon in Goldstrike ore has been shown to be congruent with the behavior of commercial activated carbon with respect to aurocyanide complex adsorption [5], increased aurocyanide complex adsorption after autoclaving may be due to an increased concentration of defects along the edges of the graphitic planes as a result of oxidation.

Although a significant increase in adsorbed gold concentration was observed for autoclaved CMs rela-

Table 3

The maximum concentration of gold possible on the natural carbon (Au_c) in Goldstrike ore during the preg-robbing test, BTAC–CIL test, and the maximum concentration of gold attributed to irreversible gold adsorption

Sample ID	Max Au_c preg-robbing test ($\mu\text{g Au/g C}$)	Max Au_c BTAC–CIL test ($\mu\text{g Au/g C}$)	Max Au_c attributed to irreversible adsorption ($\mu\text{g Au/g C}$)
BR-22	320	270	12000
PR-1G	1520	1270	7200
6th West	1100	930	4610
BTZ#3	2440	2040	2530

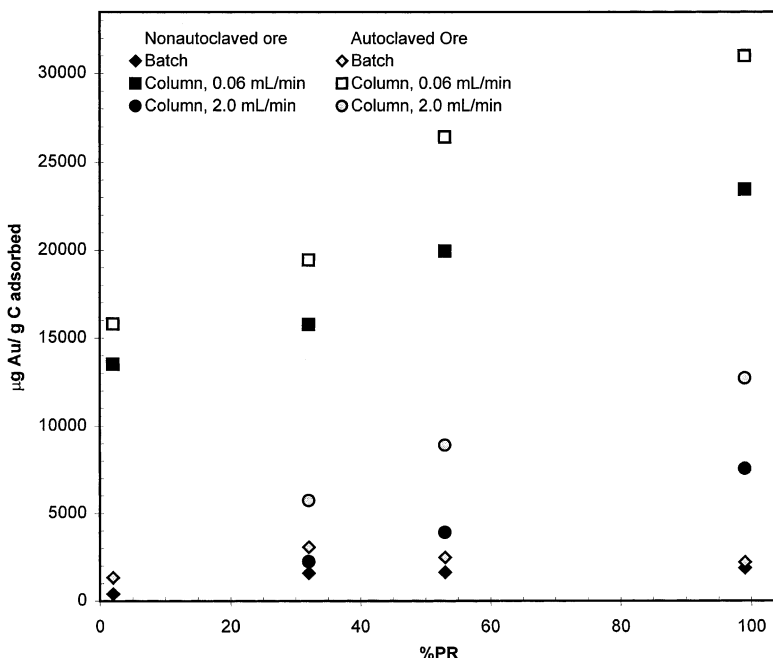


Fig. 8. Concentration of strongly adsorbed gold attributed based on gold concentrations obtained from gold adsorption from 100 mL of 10 ppm gold–cyanide solution at 0.008 mL/min and gold desorption experiments correlated with the preg-robbing behavior of the parent ore as quantified by (a) %PR and (b) %REC.

tive to the non-autoclaved CMs during the column experiments, this increase was much smaller for the batch experiments. Additionally, even the strongly preg-robbing ores showed low gold uptake in the batch experiments. The low uptake in the batch experiments may be due to the relatively small solution volume exposed to the CM (10 mL in batch vs. 100 mL in columns). Alternatively, the low adsorbed gold concentration observed in the batch experiments could be due to the much longer equilibration time for the batch (72 h) vs. column (\sim 28 h at 0.06 mL/min and \sim 1 h at 2.0 mL/min) experiments. This would be consistent with the observation that long equilibration times reduce gold adsorption (Figs. 2 and 4).

5. Discussion

5.1. Comparison of mass transfer in adsorption and desorption experiments

The flowrate at which the maximum adsorbed concentration was achieved during adsorption exper-

iments was the same for all the ores studied. The flowrate at which the minimum adsorbed concentration was achieved during desorption was also the same for all ores studied. This was not expected given the wide variation in physical and chemical properties of these CMs. This similarity may indicate that for these CMs, the properties that control the kinetics of aurocyanide adsorption are similar. In contrast, the very different adsorbed gold concentrations achieved indicate that the properties which control the overall extent of aurocyanide adsorption differ (Fig. 4).

Between the adsorption and desorption experiments, the flow rates above which $Aq \rightarrow C$ became kinetically limited (0.05 and 0.008 mL/min, respectively) and $C \rightarrow Aq$ became kinetically limited (0.008 and 0.14 mL/min, respectively) differ. This is due to differences in the driving force for mass transfer between the adsorption and desorption experiments. The driving force is equal to the difference between the gold concentrations in the aqueous and carbon phases, which differs in the adsorption and desorption experiments. For example, in the adsorption experiments, the influent aqueous gold concentration

was 10 ppm and the concentration of gold on the carbon was initially zero. In contrast, during desorption experiments, the influent aqueous gold concentration was 0 ppm and the concentration of gold on the carbon was a decreasing non-zero value.

Gold mass transfer in these experiments cannot be modeled using first order rate constants. For example, if the rate of gold mass transfer is governed by first order rate constants, then the concentration of gold on the carbon can be described by Eq. 1:

$$\frac{dAu_c}{dt} = k_{Aq \rightarrow C} \cdot Au_{Aq} - k_{C \rightarrow Aq} \cdot Au_c \\ = (Aq \rightarrow C) - (C \rightarrow Aq) \quad (1)$$

where Au_c is the concentration of gold on the carbon, Au_{Aq} is the concentration of gold in the aqueous phase, $k_{Aq \rightarrow C}$ represents the rate constant governing mass transfer from solution to carbon, and $k_{C \rightarrow Aq}$ represents the rate constant governing mass transfer from the carbon to solution. According to Eq. 1, the only means of increasing the concentration of gold on the carbon while increasing flow rate, as was observed in the adsorption experiments, is to decrease the $k_{C \rightarrow Aq} \cdot Au_c$ term, (place kinetic limitations on $C \rightarrow Aq$). However, since Au_c increased as flow rate increased above 0.008 mL/min, $k_{C \rightarrow Aq}$ must have decreased by a greater percentage to result in overall reduced $k_{C \rightarrow Aq} \cdot Au_c$. Hence, the rate constant changed with flow rate in these experiments and cannot be a simple first order constant. The same is true for the desorption experiments, where $Aq \rightarrow C$ decreased (e.g. $k_{Aq \rightarrow C} \cdot Au_{Aq}$ decreased) for flow rates above 0.008 mL/min, despite increased Au_{Aq} above this flow rate.

5.2. Potential effects of strong and weak adsorption domains on the assessment of preg-robbing behavior

In this study, it was found that the %PR and %REC values determined for the ores examined reflected gold adsorption to the strongly adsorbing domains of the carbon. Under these conditions, it can be expected that the %PR and %REC values would be complementary, that is, ores with high %PR would show low %REC, and vice versa. For other ores, however, the strong component of adsorption may be sufficiently limited to cause the %PR value to reflect both weak and strong components of ad-

sorption. In such cases, the measured %PR and %REC values would not be expected to be complementary, since commercial activated carbon added during the BTAC–CIL test would compete with the naturally occurring organic carbon. Competition with commercial activated carbon would remove weakly adsorbed gold from the naturally occurring carbon during the BTAC–CIL test, and the resulting %REC value would reflect only strongly adsorbed gold. It is possible that for ores where %REC and %PR values are not complementary, the %PR value reflects both weakly and strongly adsorbed components of adsorption, whereas the %REC value reflects only strongly adsorbed gold. Increased aurocyanide complex adsorption for autoclaved vs. non-autoclaved carbon may also obscure the relationship between measured %REC and %PR values, since the preg-robbing test uses non-autoclaved ore, whereas the BTAC–CIL test uses autoclaved ore.

The greater accuracy of the bleach leach test relative to the preg-robbing test is thought to derive from deactivation of weakly adsorbing domains of the naturally occurring carbon. It is tempting to equate the weakly adsorbing domain identified in this study to the weakly adsorbing domain that is deactivated during bleach leach tests, but for the fact that bleach leach tests are performed on non-autoclaved ores, whereas the ores examined in this study were autoclaved. Hence, additional studies are needed to determine the relationship between the weak adsorption domain observed for autoclaved ores in this study and the adsorption domain that is deactivated by the bleach leach test.

In this study, it was found that long or exceedingly short equilibration times resulted in decreased gold adsorption to naturally occurring carbonaceous matter. In order to assess whether these findings have implications for processing, additional studies should be undertaken to determine how the contact times examined here, with demineralized CM, relate to contact times used during the processing of bulk ore.

6. Conclusions

The concentration of gold adsorbed from 100 mL of gold–cyanide solution by CM depended on the

solution flow rate. Maximum gold concentrations were attained on the carbon at a flow rate of approximately 0.05 mL/min, where it is hypothesized that the mass transfer of gold from solution to the carbon was maximized while the concurrent mass transfer of gold from the carbon to solution was kinetically limited. The concentration of gold remaining on the carbon after desorption into 75 mL of sodium cyanide solution also depended on solution flow rate. Maximum desorption (minimum concentration of gold remaining on the carbon) occurred at a flow rate of approximately 0.14 mL/min, where it is hypothesized that mass transfer of gold from the carbon to solution was maximized while the mass transfer of gold from solution to the carbon was kinetically limited.

Correlation between the concentration of gold present on the carbon after minimum loading (adsorption from 100 mL gold–cyanide solution at the slowest and fastest flow rates, 0.008 and 2.0 mL/min, respectively) and the concentration of gold remaining on the carbon after maximum stripping (desorption of loaded gold at the flow rate of maximum desorption, 0.14 mL/min) suggests that strongly and weakly held components of adsorbed gold existed on the naturally occurring carbon. The concentration of gold strongly adsorbed to the carbon correlated to %PR (directly) and %REC (inversely), suggesting that this was the component of adsorption measured by preg-robbing and BTAC–CIL tests performed on these Goldstrike ores.

Non-complementary %PR and %REC values for some ores can be speculated to be due to the inclusion of weakly adsorbed gold in %PR but not %REC values, as well as increased gold adsorption by autoclaved carbon in the BTAC–CIL (%REC) test.

Acknowledgements

The authors wish to thank BGMI for providing funding and resources for this project. Additionally, thanks to the staff at BGMI Metallurgical Services for obtaining samples as well as performing fire assay and LECO analyses used in this study. Thanks to Dr. William Parry, Department of Geology and Geophysics, University of Utah, and Dr. Michael

Free, Department of Metallurgical Engineering, University of Utah for providing resources and equipment used during this study.

References

- [1] B.M. Bakken, M.F. Hochella Jr., A.F. Marshall, A.M. Turner, High-resolution microscopy of gold in unoxidized ore from the Carlin Mine, Nevada. *Economic Geology* 84 (1989) 171–179.
- [2] S. Chrysoulis, C. Weisner, C. Wong, 1996. Department of gold in composites HPR-1 and LPR-1 of Goldstrike, Barrick Goldstrike, unpublished company report, 10 pp.
- [3] D.M. Hausen, W.C. Park, Observations on the association of gold mineralization with organic matter in Carlin-type ores. in: W.E. Dean (Ed.), *Organics and Ore Deposits*. Denver Region Exploration Geologists Society, Wheat Ridge, CO, 1985, pp. 119–136.
- [4] J.D. Wells, T.E. Mullens, Gold-bearing arsenian pyrite determined by microprobe analysis, Cortez and Carlin gold mines, Nevada. *Economic Geology* 68 (1973) 187–201.
- [5] P.A. Schmitz, S. Duyvesteyn, W.P. Johnson, L. Enloe, J. McMullen, Ammoniacal thiosulfate and sodium cyanide leaching of preg-robbing Goldstrike ore carbonaceous matter, submitted to *Hydrometallurgy*.
- [6] K.G. Thomas, 1994. Research engineering design and operation of a pressure hydrometallurgy facility for gold extraction, PhD Dissertation, Delft University of Technology, CIP–Gegevens Koninklijke Bibliotheek, Den Haag, the Netherlands, 401 pp.
- [7] G.C. Smith, 1968. Discussion of refractory ore, Carlin Gold Mining, unpublished report, Feb. 20.
- [8] D.M. Hausen, C.H. Bucknam, Study of preg-robbing in the cyanidation of carbonaceous gold ores from Carlin Nevada. in: W.C. Park, D.M. Hausen, R.D. Hagni (Eds.), *Applied Mineralogy, Proceedings of the Second International Congress on Applied Mineralogy*. AIME, Warrendale, PA, 1985, pp. 833–856.
- [9] A.S. Radtke, B.J. Scheiner, Studies of hydrothermal gold deposition: (I). Carlin gold deposits, Nevada: the role of carbonaceous materials in gold deposition. *Economic Geology* 65 (1970) 87–102.
- [10] J.F. Stenebråten, W.P. Johnson, J. McMullen, Characterization of Goldstrike ore carbonaceous material: 2. Physical characteristics. *Minerals & Metallurgical Processing* 17 (2000) 1–9.
- [11] P. Butcher, J. Wilmot, Development of an analytical test to determine autoclave amenability of carbonaceous ores. CMA, SMA '98, Proceedings of the 30th Annual Conference. CMA and SMA, Kelowna, BC, 1998, pp. 154–171.
- [12] R. Dix, 2000. BGMI Metallurgical Services, Carlin, NV, Personal Communication, June 2000.
- [13] G.J. McDougall, R.D. Hancock, Gold complexes and activated carbon: a literature review. *Gold Bulletin* 14 (1981) 138–153.

- [14] J.H. Nelson, J.J. MacDougal, F.G. Baglin, D.W. Freeman, M. Nadler, J.L. Hendrix, Characterization of Carlin-type gold ore by photoacoustic, Raman and EPS spectroscopy. *Applied Spectroscopy* 36 (1982) 574–576.
- [15] P.L. Sibrell, R.Y. Wan, J.D. Miller, Spectroscopic analysis of passivation reactions for carbonaceous matter from Carlin trend ores. *Gold '90, SME Symposium*, Salt Lake City, UT, 1990, pp. 355–363.
- [16] J.F. Stenebråten, W.P. Johnson, J. McMullen, Characterization of Goldstrike ore carbonaceous material: 1. Chemical characteristics. *Minerals & Metallurgical Processing* 16 (1999) 37–43.
- [17] M.D. Adams, 1989. The chemistry of the carbon-in-pulp process, PhD Dissertation, University of the Witwatersrand, Johannesburg, South Africa, 387 pp.
- [18] N.P. Gallagher, J.L. Hendrix, E.B. Milosavljevic, J.H. Nelson, L. Solujic, Affinity of activated carbon towards some gold (I) complexes. *Hydrometallurgy* 25 (1990) 305–316.
- [19] M.D. Adams, G.J. McDougall, R.D. Hancock, Models for the adsorption of aurocyanide onto activated carbon: Part 2. Extraction of aurocyanide ion pairs by polymeric adsorbents. *Hydrometallurgy* 18 (1997) 139–154.
- [20] M.D. Adams, G.J. McDougall, R.D. Hancock, Models for the adsorption of aurocyanide onto activated carbon: Part 3. Comparison between the extraction of aurocyanide by activated carbon, polymeric adsorbents and 1-Pentanol. *Hydrometallurgy* 19 (1987) 95–114.
- [21] A.S. Ibrado, D.W. Fuerstenau, Infrared and X-ray photoelectron spectroscopy studies on the adsorption of gold-cyanide on activated carbon. *Minerals Engineering* 8 (1995) 441–458.
- [22] C. Klauber, X-ray photoelectron spectroscopic study of the adsorption mechanism of aurucyanide onto activated carbon. *Langmuir* 7 (1991) 2153–2159.
- [23] G.J. McDougall, M.D. Adams, R.D. Hancock, Models for the adsorption of aurocyanide onto activated carbon: Part 1. Solvent extraction of aurocyanide ion pairs by 1-Pentanol. *Hydrometallurgy* 18 (1987) 125–138.
- [24] P.L. Sibrell, J.D. Miller, Significance of graphitic structural features in gold adsorption by carbon. *Minerals & Metallurgical Processing* 9 (1992) 189–195.
- [25] J.D. Miller, P.L. Sibrell, Nature of gold adsorption from cyanide solutions by carbon. in: D.R. Gaskell (Ed.), EPD Congress '91, The Minerals Metals and Materials Society, 1991, pp. 647–663.
- [26] P.L. Sibrell, 1991. The characterization and treatment of Carlin trend carbonaceous gold ores, PhD Dissertation, University of Utah, Salt Lake City, UT 196 pp.
- [27] S. Lagerge, J. Zajac, S. Partyka, A.J. Groszek, M. Chesneau, Adsorption of cyanide gold complexes inferred from various experimental studies. *Langmuir* 13 (1997) 4683–4692.
- [28] S. Lagerge, J. Zajac, S. Partyka, A.J. Groszek, Comparative study on adsorption of cyanide gold complexes onto different carbonaceous samples: measurement of the reversibility of the process and assessment of the active surface inferred by flow microcalorimetry. *Langmuir* 15 (1999) 4803–4811.